International Journal of Engineering & Technology, 7 (4.39) (2018) 743-749

International Journal of Engineering & Technology

Website: www.sciencepubco.com/index.php/IJET

Research paper



Modified OFDM Receiver Design with Improved Channel Capacity

R. Anil Kumar [1], Dr. K. Satya Prasad [2]

[1] *Assistant Professor, Electronics and Communication Engineering,* Surampalem, Andhra Pradesh, India.
[2] *Pro Vice-Chancellor* of K L University, Vijayawada, Andhra Pradesh, India.
**Corresponding author Email: anidecs@gmail.com, prasad_kodati@yahoo.co.in*

Abstract

High data transmission rate, reliability and spectral efficiency are necessary for developing wireless communication systems for real time seamless audio and video transmission. To find the impact of wireless channel on OFDM signal, channel estimation plays a major role. In this paper, implementation of pilot assisted channel estimation and performance analysis of the CFO and STO are investigated and estimated. Distinctive channel estimation techniques like Least Square (LS), Minimum Mean Square Error estimator (MMSE) and proposed MMSE strategies are discussed and furthermore, this paper focuses on performance juxtaposition of the channel, CFO and STO estimation with reference to Symbol error rate and Mean square error. If the mean square error is higher for low SNR sub-channels, then allocate power by using water filling algorithm to increase the channel capacity of the users.

Keywords *: OFDM, CFO, STO, LS, MMSE, Channel Capacity, Water-filling*

1. Introduction

OFDM systems have become more and more fashionable in wireless broadcasting because of its high rate and quality transmission capability and its ability to inhibit multipath de- lay. Future wireless communications require more bandwidth and higher data rates. High bandwidth is often impossible because of spectral limitations. OFDM encounters requirement of evolving wireless channel capacity using accessible band- width and diminish inter-symbol interference. Fig. 1 shows the OFDM transceiver. OFDM is a multi-carrier multiplexing and employs digital modulation system that splits the complete channel into various parallel sub-channels, so that it eliminates inter symbol interference (ISI) and increases data rate.

The basic principle of OFDM is converts high rate serial bit stream into low rate parallel bit stream. Here channel will be considered as flat-tapped channel due to parallel bit streams. The sub- carriers in OFDM are overlapped and orthogonal to each other. These basic characteristics reduces the significant inter symbol interference (ISI) and increase the spectral efficiency of receiving OFDM signals. The sub-carriers are separated by guard band and not overlapped in FDM, which will decrease the spectral efficiency of signal. Orthogonality of carrier can be attained by selecting appropriate spacing of the carrier to be the reciprocal of the symbol time. A frequency wideband channel has converted into a group of narrow band channels in OFDM system. The applications of the proposed work are to solve channel capacity and data rate issues in advanced communication systems like cognitive radio communication systems, multiple-input multiple-output communication systems and green communication systems [1-2].

There are two categories of distortions accompanied by the carrier signal which are the carrier frequency offset (CFO) and symbol time offset (STO). OFDM system has more sensitivity to devices. Environmental factors result in timing and carrier frequency errors which are more than a single carrier modulation system. A delay in the channel impulse response modelled as Symbol timing offset and difference in local oscillator frequencies in the transmitter and receiver modelled as carrier frequency offset which gives rise to shift in the frequency of receiving signals. Due to shrinkage in orthogonality among sub-carriers, the carrier frequency offset arises. Both STO and CFO represented phase rotation while exclusively STO represented as inter-symbol interference (ISI) and CFO as inter-channel interference (ICI) [2-3].

Equations (1) and (2) conveys the detected signal under the influence of CFO and STO where normalized CFO and STO denotes (ε) and ((δ)) respectively.

$$y_l[\mathrm{n}] = \mathrm{IDFT}\{Y_l[\mathrm{k}]\} = \mathrm{IDFT}\{H_l[\mathrm{k}]X_l[\mathrm{k}] + Z_l[\mathrm{k}]\} \quad (1)$$

$$= \frac{1}{N}\sum_{k=0}^{N-1} H_l[\mathrm{k}]X_l[k]e^{\frac{j2\pi(K+\varepsilon)(n+\delta)}{N}} + z_l[\mathrm{n}] \quad (2)$$

Copyright © 2018 Authors. This is an open access article distributed under the Creative Commons Attribution License, which permits unrestricted use, distribution, and reproduction in any medium, provided the original work is properly cited.

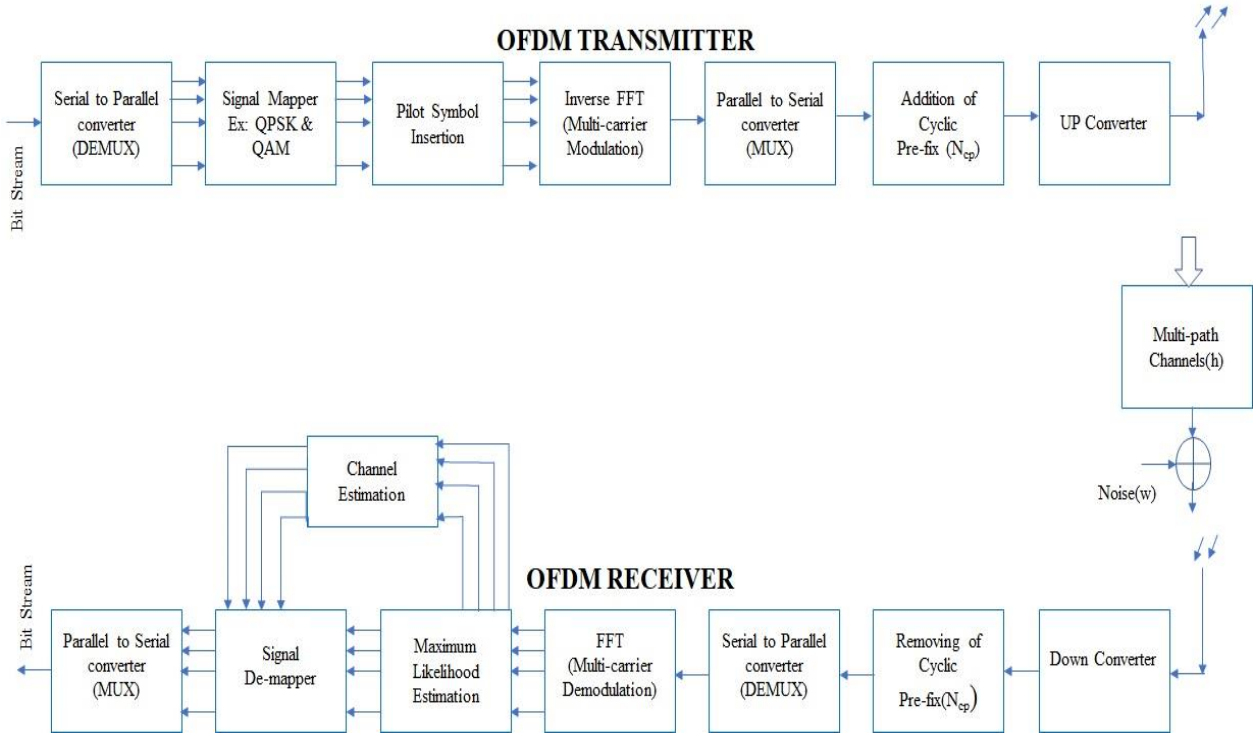


Fig. 1: OFDM Trans-receiver with STO, CFO and channel estimation

2. Analysis of STO, CFO and Channel Effects of OFDM system

Symbol time offset

In order to perform the modulation and demodulation in OFDM system, Inverse Fast Fourier Transform (IFFT) and Fast Fourier Transform (FFT) functions are applied at the transmitter and receiver. The explicit samples of the transmitted signal are entailed for the symbol duration (T) of the OFDM to perform the N point Fast Fourier Transform in the receiver. The receiver receives exact samples if there is a symbol timing synchronization for detection of each OFDM symbol. In frequency and time domain the received symbols are affected the samples by the STO. In the frequency domain, the phase offset of $\frac{2\pi\delta k}{N}$ occurs due to the STO of δ in the time domain which depends on the STO δ and subcarrier index k. The position of the estimated origin of OFDM symbol incurs the backlash of STO.

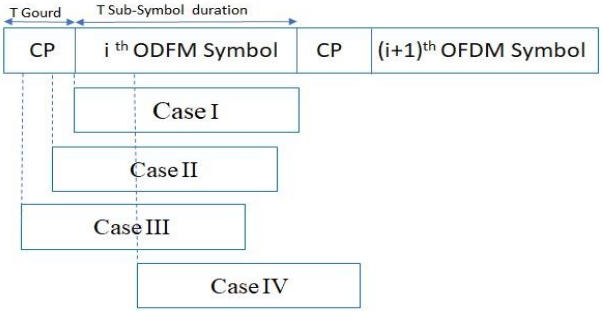


Fig. 2 : Origin of OFDM symbol for différent cases subjected to STO

Assume the maximum channel delay spread and timing offset are τ_{max} and δ respectively. Sample indexes of perfectly synchronized OFDM symbols are represented with $-N_G \ldots -1,0,1 \ldots \ldots N-1$. By taking the FFT of time domain received samples $\{x_l[n+\delta]\}_{n=0}^{N-1}$ at the FFT output in every subcarrier a phase rotation is introduced by the timing offset given as T_G as shown in Fig. 2. When $\delta \in -N_G \ldots -1,0,1 \ldots \ldots N-1$, the orthogonality between the subcarriers is indestructible and a phase rotation is introduced by the timing offset in every subcarrier symbol at the Fast Fourier Transform output after taking the Fast Fourier Transform of the time domain received samples $\{x_l[n+\delta]\}_{n=0}^{N-1}$ as T_G [3].

$$X_l[\mathrm{k}] = \frac{1}{N}\sum_{n=0}^{N-1} x_l[\mathrm{n}+\delta]\, e^{-\frac{j2\pi nk}{N}} \tag{3}$$

$$= X_l[\mathrm{k}]\frac{ej2\pi k\delta}{N} \tag{4}$$

Inter symbol interference (ISI) and additional inter carrier interference (ICI) arises due to the shrinkage in orthogonality among the subcarriers, whenever the timing estimate is beyond the starting point of OFDM symbol.

Then the ICI is derived as followed:

$$Y_l[\mathrm{k}] = \sum_{n=0}^{N-1-\delta}\left(\frac{1}{N}\sum_{p=0}^{N-1} X_l[\mathrm{p}]e^{\frac{j2\pi(n+\delta)p}{N}}\right)e\frac{-j2\pi nk}{N} + \sum_{n=N-\delta}^{N-1}\left(\frac{1}{N}\sum_{P=0}^{N-1} X_{l+1}[\mathrm{p}]e^{\frac{j2\pi p(n+2\delta-N_g)}{N}}\right)e\frac{-j2\pi nk}{N} \tag{5}$$

$$Y_l[\mathrm{k}] = \frac{N-\delta}{N}X_l[\mathrm{p}]\frac{e^{j2\pi p\delta}}{N} + \sum_{p=0,p\neq k}^{N-1} X_l[\mathrm{p}]e^{\frac{j2\pi p\delta}{N}}\sum_{n=0}^{N-1-\delta} e\frac{j2\pi(p-k)n}{N} + \frac{1}{N}\sum_{P=0}^{N-1} X_{l+1}[\mathrm{p}]e^{\frac{j2\pi p(2\delta-N_g)}{N}}\sum_{n=N-\delta}^{N-1} e\frac{j2\pi(p-k)n}{N} \tag{6}$$

Where,

$$\sum_{n=0}^{N-1-\delta} e\frac{j2\pi(p-k)n}{N} = e^{j\pi(p-k)}\frac{N-1-\delta}{N}\frac{\sin[\frac{(N-\delta)\pi(k-p)}{N}]}{\sin[\frac{\pi(k-p)}{N}]} = \begin{cases}\mathrm{N}-\delta & \text{for p = k}\\ \text{finate} & \text{for p} \neq k\end{cases} \tag{7}$$

Here, ICI and received signal which involves ISI corresponds to the second and the third term in Equation (6) respectively.

Carrier Frequency Offset

CFO, which is induced by Doppler frequency shift f_d.Transmitter and receiver carrier frequencies are denoted by $f_c$and f_c' which are differed by f_{offset}, where$f_{offset} = f_c - f_c'$.The ratio of f_{offset} to the subcarrier spacing ∇f stated as normalized CFO ε as shown Fig. 3.

$$\varepsilon = \frac{f_{offset}}{\Delta f} \tag{8}$$

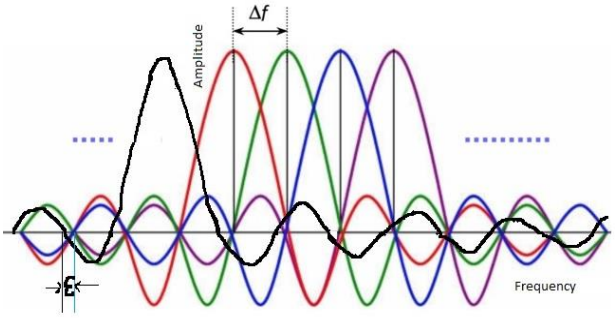


Fig. 3: Carrier Frequency Offset among the subcarriers

A phase shift of 2πnε depends on the time index n and CFO for the received time domain signal x[n] can be written as

$$y_l[\mathrm{n}] = \frac{1}{N}\sum_{K=0}^{N-1} H[\mathrm{k}]X_l[\mathrm{k}]\, e^{j2\pi(k+\varepsilon)n/N} + Z_l[\mathrm{n}] \tag{9}$$

The normalized CFO categorized into fractional CFO (FFO) ε_f and integer CFO (IFO) ε_i that is $\varepsilon = \varepsilon_f + \varepsilon_i$, because of the IFO, the transmitted signal X[k]is cyclically shifted by $\varepsilon_i$in the receiver, and thus producing X[k $-\varepsilon_i$] in the k^{th} subcarrier. A significant deterioration in the Bit Error Rate performance will occur until the cyclic shift is uncompensated. ICI will not occur if there is no loss of orthogonality between the subcarrier frequency samples [3]. The received frequency domain signal with an FFO of $\varepsilon_f$can be written as

$$Y_l[\mathrm{k}] = \frac{\sin(\pi\varepsilon_f)}{N\sin\pi\varepsilon_f/N} e^{\frac{j\pi\varepsilon_f(N-1)}{N}} \mathrm{H[k]}X_l[\mathrm{k}]l_l[\mathrm{k}] + Z_l[\mathrm{k}] \tag{10}$$

$$l_l[\mathrm{k}] = e^{\frac{j\pi\varepsilon_f(N-1)}{N}} \sum_{m=0,m\neq k}^{N-1} \frac{\sin\left(\pi\left(m-k+\varepsilon_f\right)\right)}{N\sin\left(\frac{\pi\left(m-k+\varepsilon_f\right)}{N}\right)} \mathrm{H[m]}X_l[\mathrm{m}]\, e^{\frac{j\pi(m-k)(N-1)}{N}} \tag{11}$$

In Equation (10) The phase and amplitude distortion of the k^{th}subcarrier frequency component caused by FFO, while $l_l[\mathrm{k}]$ gives the ICI from alternative subcarriers into k^{th} subcarrier frequency component, which shows the destroyed orthogonality among the subcarriers. Fig. 4 shows the normalized CFO versus the magnitude of error difference in dB.

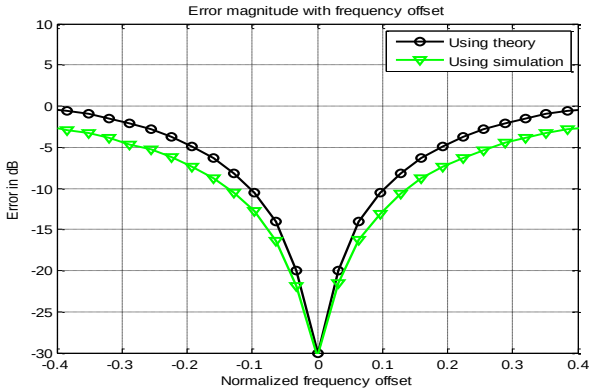


Fig. 4: Error in magnitude to normalized CFO

Channel Effect

Substantially, the channel estimation of OFDM systems can be estimated by channel frequency response. The Channel estimation is categorized into two types namely training-based channel estimation and Blind channel-based estimation. Certain properties of the transmitted signal and channel statistical information are used in Blind channel estimation. This channel estimation is pertinent to slowly time-varying channels and it does not contain overhead loss [4]. Whereas, in training-based estimation pilot symbols are used which are known at receiver and transmitter. To get the efficient channel estimation more number of pilot symbols required but which increases the overhead of transmitted data. This paper presents only on training-based channel estimation technique of two types namely comb type and block type arrangement.

Comb Type Pilot Arrangement

In this category subcarriers carry pilot tones in each and every OFDM symbol. Duration of the pilot symbol is denoted by S_f which related with coherence time as shown in equation (11).

$$S_f \leq \frac{1}{\sigma_{max}} \tag{11}$$

Block Type Pilot Arrangement

At a time, all subcarriers are multiplexed with pilot symbols which are transmitted periodically in this Block type Pilot arrangement. Here the pilot symbol duration is denoted by S_t and related with doppler frequency $f_{Doppler}$ as shown in equation (12)

$$S_t \leq \frac{1}{f_{Doppler}} \tag{12}$$

3. Estimation of STO, CFO and Channel in OFDM System

1. Estimation of symbol timing offset

Both the ISI and STO causes phase distortion in OFDM. By using synchronization technique at receiver end, the initial point of OFDM symbols are estimated to improve the performance. Assume the effective data samples $\boldsymbol{N_{SUB}}$ over $\boldsymbol{T_{SUB}}$ seconds and cyclic prefix (CP) samples $\boldsymbol{N_G}$over $\boldsymbol{T_G}$ seconds. CP or training symbols methods used for estimation of STO in time domain [5-6].

Estimation of STO Using CP

CP is the exact part of OFDM symbol based on this similarity CP is used for estimation of STO.W_1 and W_2 are spaced by NSUB samples are the two sliding windows which are taken as corresponding data part and CP part as shown in Fig. 5. The sliding of these windows used to find correlation among the samples within W_1 and W_2.

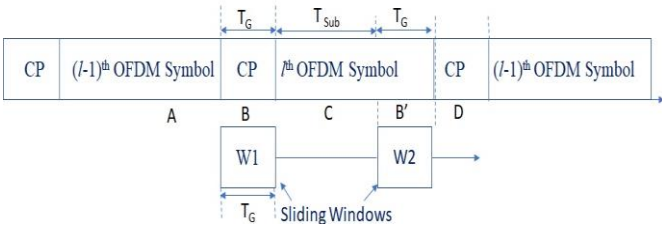


Fig. 5: STO estimation technique using Cyclic Prefix

When CP of an OFDM symbol matched with the first sliding window then W_1 and W_2 results in maximum correlation. Hence the difference between the two blocks of windows is minimized that is shown in equation (13).

$$\hat{\delta} = \arg\min_{\delta}\left\{\sum_{i=\delta}^{N_G-1+\delta}|y_l[n+i]-y_l[n+N+i]|\right\} \quad (13)$$

CFO degrades the OFDM system performance. The minimization of the squared difference between the conjugate of N_G (window W_2) sample block and another N_G (window W_1) sample block in the STO estimation method.

$$\hat{\delta} = \arg\min_{\delta}\left\{\sum_{i=\delta}^{N_G-1+\delta}(|y_l[n+i]-y_i{}^*[n+N+i]|)^2\right\} \quad (14)$$

The maximum-likelihood estimation method is shown as in equation (15) in which sliding windows correlation used for STO estimation.

$$\hat{\delta} = \arg\max_{\delta}\left\{\sum_{i=\delta}^{N_G-1+\delta}(|y_l[n+i]y_l{}^*[n+N+i]|)\right\} \quad (15)$$

To maximizes the above equation maximum log likelihood functions are applied

$$\hat{\delta}_{ML} = \arg\max_{\delta}\sum_{i=0}^{N_G-1+\delta}[2(1-p)Re\{y_l[n+i]y_l{}^*[n+N+i]\}] - \arg\max_{\delta}\sum_{i=0}^{N_G-1+\delta}\left[p\sum_{i=0}^{N_G-1+\delta}|y_l[n+i]-y_l[n+N+i]|\right] \quad (16)$$

By using ML estimation technique both STO and CFO can be estimated at same time Where, $= \frac{SNR}{SNR+1}$. Symbol time offset is estimated as follows

$$\hat{\delta}_{ML} = \arg\max_{\delta}\{|\gamma[\delta]| - \rho\Phi[\delta]\} \quad (17)$$

Where,

$$\gamma[m] = \sum_{n=m}^{m+L-1} y_l[n]y_l{}^*[n+N] \quad (18)$$

And

$$\Phi[\mathrm{m}] = \frac{1}{2}\sum_{\mathrm{n=m}}^{\mathrm{m+L-1}}\{|\mathrm{y_l[n]}|^2 + |\mathrm{y_l[n+N]}|^2\} \quad (19)$$

Average samples in windows are denoted with L. Equation (18) estimates the STO by exalting the correlation between part of OFDM symbol and corresponding cyclic prefix whereas equation (17) estimates by depreciating the difference between a part of OFDM symbol and cyclic prefix. The simulation results are calculated for STO by fixing CFO at 0.00 and 0.50. The maximum correlation occurs for estimated STO values such as -3 and 2 for received symbols illustrated in Fig. 6

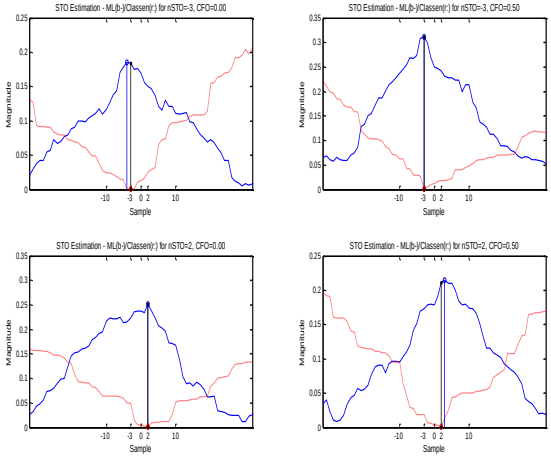


Fig. 6: Performance of maximum correlation and minimum difference estimation for different STO values.

Estimation of STO using frequency domain approach

Phase difference introduced among the neighbouring subcarrier components of the received signal to estimate the STO in the frequency domain [6]. When $X_l[k] = X_l[k-1]$ and $H_l[k] = H_l[k-1]$for all k then $Y_l[k]Y_l^*[k-1] = |X_l[k]|^2 e^{\frac{j2\pi\delta}{N}}$. STO estimation is given by

$$\hat{\delta} = \frac{N}{2\pi} arg\left(\sum_{k=1}^{N-1} y_l[k]y_l{}^*[k-1]\right) \quad (20)$$

The conjugated training symbol $X_l^*[k]$ is multiplied with the received symbol (with STO) to obtain channel impulse response which is used to estimate the STO

$$\hat{\delta} = \arg\max_{n}(y_l{}^*[n]) \quad (21)$$

Where, $y_l{}^*[n] = IFFT\left\{y_l[k]e^{\frac{j2\pi k\delta}{N}}X_l{}^*[k]\right\} = h_l[n+\delta]$ (22)

The mean square value of training symbol $X_l[k]$ is equal to unity ($X_l[k]X_l^*[k] = |X_l[k]|^2 = 1$) Channel impulse response is used for STO estimation, Simulation results as shown in Fig. 7. As per the simulation results, samples are shifted around the reference point by fixing CFO values at 0.00 and 0.50 to estimate STO at -3 and 2.

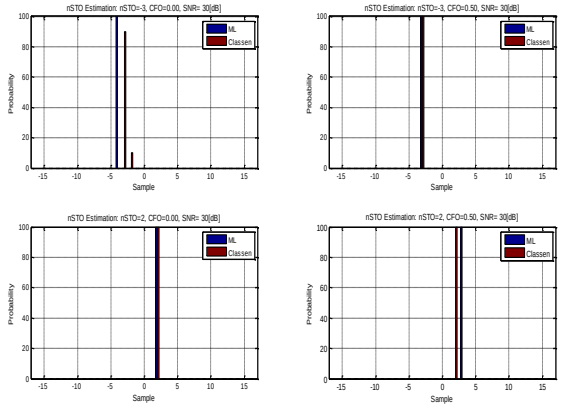


Fig. 7: Performance of STO in frequency domain estimation.

2. Estimation of CFO

A significant degradation in performance occurs due to frequency mismatch between oscillator frequency and received frequency in

OFDM system. Both time and frequency domain are used to estimate the CFO [5-6].

Estimation of CFO Using CP

At the receiver a phase rotation of $\frac{2\pi n\varepsilon}{N}$ caused by CFO. A phase difference between a part of OFDM symbol and the corresponding part of CP occurred due to CFO. Multiplication of CP and real part of OFDM symbol used to estimate CFO as equation (23)

$$\hat{\varepsilon} = (1/2\pi) arg\{y_l^*[n] y_l[n+N]\} \quad (23)$$

The average samples as in CP interval is given by

$$\hat{\epsilon} = \frac{1}{2\pi} arg\left\{\sum_{n=-N_G}^{-1} y_l^*[n] y_l[n+N]\right\} \quad (24)$$

CFO estimation lies in the range of $[(-\pi, \pi)/2\,\pi] = [-0.5+0.5]$ so that $|\varepsilon| < 0.5$. When there is no frequency offset the term $y_l^*[n] y_l[n+N]$ becomes real and imaginary if there is CFO. Here imaginary part of $y_l^*[n] y_l[n+N]$ applied for CFO estimation and error is given by

$$e_\varepsilon = \frac{1}{L}\sum_{n=1}^{L} I_m\{y_l^*[n] y_l[n+N]\} \quad (25)$$

Where L denotes the average samples. The mean value of error function given as equation (26)

$$E\{e_\varepsilon\} = \frac{{\sigma_d}^2}{N} sin\left(\frac{2\pi\varepsilon}{N}\right)\sum_k^L |H_k|^2 \approx K_\varepsilon \quad (26)$$

The Impulse response of the channel and transmitted signal power are H_k and ${\sigma_d}^2$ respectively.

Estimation of CFO using Training Symbol

At initial synchronization stage the CFO estimation range will be large but when using CP based technique, the range is between range $|\hat{\epsilon}|$ <0.5. By the reduction of the distance between samples in two windows for correlation the estimation range of CFO will be effected, this is possible if the training symbols are repetitive with a shorter period [6]. After taking IFFT at the transmitter the repetitive patterns in time domain D which denoted ratio of the length of OFDM symbol to repetitive pattern length as shown in equation (27)

$$X_l[k] = \begin{cases} A_m, & if\ \ k = D.i, i = 0,1 \ldots (\frac{N}{D} - 1) \\ 0, & otherwise \end{cases} \quad (27)$$

and A_m represents integer and M-ary symbol respectively. CFO can be estimated as shown in equation (28) when $x_l[n]$and $x_l[n + N/D]$ are identical.

$$\hat{\epsilon} = \frac{D}{2\pi} arg\left\{\sum_{n=0}^{\frac{N}{D}-1} y_l^*[n] y_l[n+\frac{N}{D}]\right\} \quad (28)$$

The CFO estimation range is $\{|\varepsilon| < D/2\}$. Mean square error performance becomes poor when estimation range of CFO increases.

Estimation of CFO using frequency domain approach

The received signal effected with CFO (ε) when two same timing symbols are transmitted then they are related as

$$y_2[n] = y_1[n] e^{\frac{j2\pi N\varepsilon}{N}} \ and\ \ Y_2[k] = Y_1[k] e^{2\pi\varepsilon} \quad (30)$$

The CFO can be estimated as

$$\hat{\varepsilon} = \frac{1}{2\pi} arg \sum_{k=0}^{N-1} Im\left[Y_1^*[k] Y_2[k]\right] / \sum_{k=0}^{N-1} Re\left[Y_1^*[k] Y_2[k]\right] \quad (31)$$

In general synchronization process categorized tracking and acquisition phases, in tracking mode the residual small deviations are corrected where as a rough estimate of CFO calculated and corrected in acquisition phase. In real time systems conditions are dynamic causes small deviation in CFO hence tracking method should estimate and correct the CFO. This approach is proposed by Moose [7]. The CFO estimation range is $|\varepsilon| \leq \frac{\pi}{2\pi} = 1/2$. The other method is given by Classen [12] where in each OFDM symbol pilot tones are inserted for CFO tracking in frequency domain. The SNR is calculated in terms of estimated CFO as shown in equation (32).

Where, $$\text{SNR} = \frac{\mathrm{P}|\mathrm{h}|^2\left(\frac{\mathrm{Sin}(\pi\hat{\epsilon})}{\pi\hat{\epsilon}}\right)}{0.822\mathrm{P}|\mathrm{h}|^2\{\mathrm{Sin}(\pi\hat{\epsilon})\}^2+\sigma_n^2} \quad (32)$$

From equations (24),(28),(31) and (32) CFO can be plotted as shown in Fig. 8 by using the phase difference between a part of OFDM symbol and corresponding cyclic prefix, using phase differences among two repetitive preambles and pilot tones in two OFDM symbols.

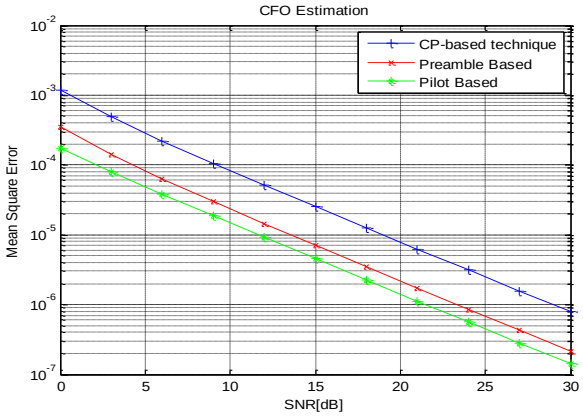


Fig. 8: Performance of CFO estimation for different methods.

Therefore, as SNR of the received signal increases the mean square of CFO estimation error gradually decreases. Here the pilot-based CFO estimation shows performance when compared to other estimation methods. The factors effecting the performance of CFO estimation are number of pilot tones, number of samples in preamble and length of the cyclic prefix

.

2.

3.

3. Channel Estimation

The quality of the received signal depends on the channel characteristics, where channel estimation plays a major role to decode received signal in coherent detection [7]. Here $g(t)$ denotes the channel response as shown below

$$g(t) = \sum_m \alpha_m \delta(t - \tau_m T_s) \quad (33)$$

Complex multipath gain and period of OFDM symbol represents α_m, T_s respectively. Equation (34) gives the received signal.

$$Y = FFT[IFFT(X) * g + n] \quad (34)$$

Where, $X = [x_0\, x_1 \ldots x_{N-1}]^T$ and $Y = [y_0\, y_1 \ldots y_{N-1}]^T$ are transmitted vector and received vector respectively, $n = [n_0\, n_1 \ldots n_{N-1}]^T$ is Additive white Gaussian Noise(AWGN) samples, $G = [g_0\, g_1 \ldots g_{N-1}]^T$ is frequency response samples of $g(t)$ can be notated in the matrix form as follows:

$$Y = XFg + Fn \quad (35)$$

The FFT matrix represented as:

$$F = \begin{bmatrix} W_N^{00} & \cdots & W_N^{0(N-1)} \\ \vdots & \ddots & \vdots \\ W_N^{(N-1)0} & \cdots & W_N^{(N-1)(N-1)} \end{bmatrix} \quad (36)$$

Where, $W^{nk} = \frac{1}{\sqrt{N}} e^{\frac{-j2\pi kn}{N}}$ is twiddle factor

7By depreciating the squared error between the received signal and estimated value which helps to find channel estimation in the least-square estimator [8-9]. Therefore, LS method is simple and widely used. $(Y - XH)^*(Y - XH)$ is a cost function minimized by estimator [10] and given as

$$\mathcal{H}_{LS} = X^{-1}Y \quad (37)$$

Minimum mean square error $MSE_{LS} = \frac{\sigma_n{}^2}{\sigma_x{}^2}$

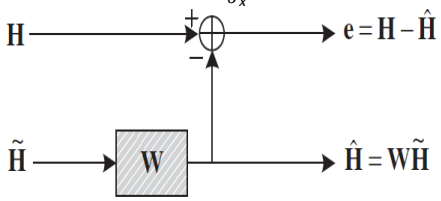


Fig. 9: Minimum mean square estimator

Whereas Minimum Mean Square Error (MMSE) gives better estimation as shown Fig. 9 while using Weights (W) in given minimized equation (38) as shown below:

$$\mathcal{H}_{MMSE} = R_{H\mathcal{H}} \left(R_{HH} - \frac{\sigma_n{}^2}{\sigma_x{}^2} I \right)^{-1} \mathcal{H} \quad (38)$$

For fading channels, Jake's spectrum in time domain correlation $r_t(l) = J_o(2\pi f_{\max} l T_{sys})$. Where $T_{sys} = T_{sub} + T_G$ and maximum doppler frequency (f_{max}) for first kind of 0^{th}-order Bessel function. Frequency domain correlation is $\gamma_f = \frac{1}{1 + j2\pi\tau_{rms} k\Delta f}$. Here, Fig. 10 present the performance of channel estimation of various techniques. Where modified LS and MMSE gives better estimation for instance at 40dB SNR the mean square error approximately equals 10^{-6}.

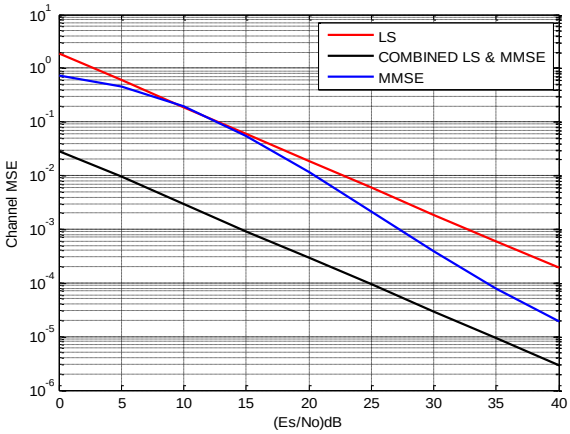


Fig. 10: Performance of frequency channel estimation for different techniques

4. Water filling algorithm for above estimated OFDM signal

The water-filling algorithm gives a better solution to maximize the average mutual information between output and input of channel consisting of several sets of parallel sub-channels for global power limitation at the transmitter. In OFDM systems to maximize the channel capacity by allocating optimal power to users is known as the water-filling algorithm. This algorithm provides an efficient solution to many constrained optimization problems in engineering. It can be visually interpreted as a tank filled by pouring water where the bottom of the tank gives inverse sub-channel gains as shown in Fig. 11, thus the name water pouring or water-filling [11-12].

Generally, expression for water filling $P_i = (\mu a_i - d_i)^+$ where a_i's and d_i's gives the visual interpretation of variables $\widetilde{P}_i = P_i/a_i$, $h_i = a_i/d_i$ resulting in weighted power constraint gives the expression $\sum_i \widetilde{P}_i w_{i=} P_t$, width of the each sub channel represented by weights w_i & a_i.

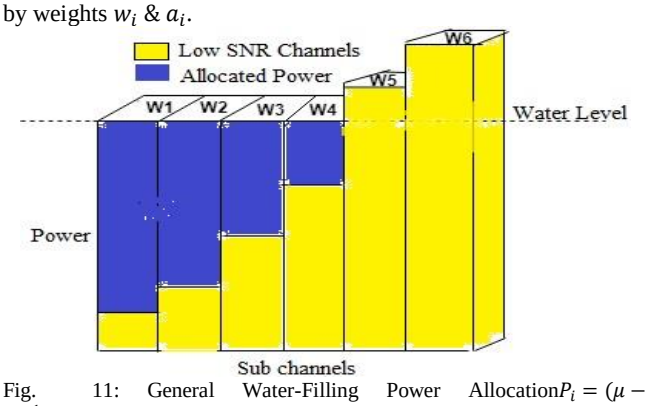


Fig. 11: General Water-Filling Power Allocation $P_i = (\mu - h_i{}^{-1})^+ with \sum_i P_i w_i = P_t$

In general, the water-filling problem can be modelled and generalized as follows: The total power (volume of water) assumed as $P_t > 0$ whereas i^{th} channel gives h_i and P_i are propagation path channel gain and allocated power for i^{th} channel respectively. Where $i = 1 \ldots N$; and N denotes the total number of sub-carriers. The sequence of channel gains denoted with $\{h_i\}_{i=1}^N$ which is monotonically decreasing and positive [13-14]. The maximum rate for reliable communication.

$$C = \sum_{n=0}^{N-1} \log\left(1 + \frac{P_i |h_i|^2}{N_0}\right) \quad (37)$$

To maximize the bit rate in above equation the power allocation is the solution to the optimization problem.

$$C_i = \max_{P_{0\ldots,} P_{N-1}} \sum_{n=0}^{N-1} \log\left(1 + \frac{P_i |h_i|^2}{N_0}\right) \quad (38)$$

$$\sum_{i=1}^{N} P_i = P_t, \quad (39)$$

The Karush-Kuhn-Tucker (KKT) proposed a better solution for the above problem by using a group of optimal conditions derived from equation (39) as shown below

$$\begin{cases} P_i = \left(\mu - \frac{1}{h_i}\right)^+, for\ i = 1, \ldots, N, \\ \sum_{i=1}^{N} P_i = P_t, \\ \mu \geq 0, \end{cases} \quad (40)$$

To satisfy the power sum constraint with equality $\sum_{i=1}^{N} P_i = P_t$ the parameter μ is to be chosen. Above equation gives the convex solution, to acquire the optimal solution so that the perseverance of its Lagrange multipliers determines the utilized water level μ.

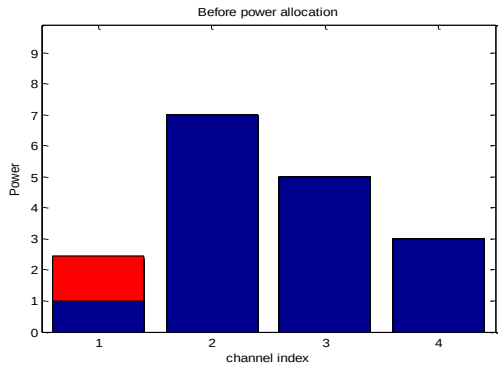


Fig. 12: Before Water-Filling Power Allocation to the sub channels

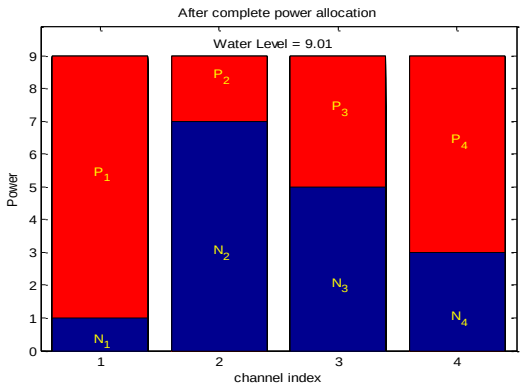


Fig. 13: After complete Water-Filling Power Allocation to the wireless sub channels

Here, Fig. 12 and Fig. 13 shows power allocation to the sub-channels before and after the application of water-filling algorithm in the noise scenario. More power is allocated to the subcarrier in the high noise scenario N_1(low SNR) and capacity is also increased by using the water-filling algorithm. Fig. 14 gives the detailed description of channel capacity versus SNR where signal to noise ratio is directly proportional to channel capacity therefore, the outage probability of user connectivity is decreased. By proposed water-filling algorithm there is a significant increase in channel capacity that is user connectivity increases when compared to classical power allocation.

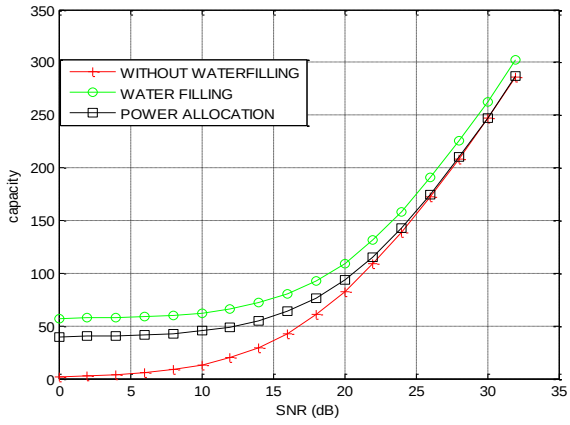


Fig. 14: Channel capacity for various power allocation techniques

5. Conclusions

This paper proposes the performance of channel estimation, frequency and timing offsets by MATLAB simulation. According to simulation results, samples are shifted around the reference point based on values of STO and CFO. For different methods of CFO estimation where SNR of the received signal increases the mean square of CFO estimation error gradually decreases and also evaluated the performance of LS, MMSE, proposed estimation for OFDM systems (LTE Downlink Systems) under the influence of channel effect. In order to avoid the ISI and ICI, the length of CP is chosen as equal or more than the channel length. Ultimately, power is allocated to the low SNR wireless sub-channels in noise environment by using Water filling algorithm to achieve good channel capacity. Simulation Results represents, Number of end user's connectivity increases from 30 to 80 users at SNR $15dB$.

6. References

[1] E. Ahmed, W. Aziz, S. Saleem, Q. Islam, Performance Analysis of OFDM System for Different Channel Lengths and Multipath Channel Taps, Advances in Electrical Engineering Systems (AEES), Vol: 1, No. 2, 2012, pp.124-128.

[2] SC HMIDL, T. M., COX, D. C. Robust frequency and timing synchronization for OFDM. IEEE Transactions on Communications, 1997, vol. 45, no. 12, p. 1613 – 1621.

[3] MORELLI, M., MENGALI, U. An improved frequency offset estimator for OFDM applications. IEEE Communications Letters, 1999, vol. 3, no. 3, p. 75 – 77.

[4] P.V.NAGANJANEYULU, K.SATYAPRASAD, "Adaptive Channel Estimation in OFDM System Using Cyclic Prefix (Kalman Filter Approach)" written published by International Journal of Communications, Network and System Sciences, Vol.2 No.9, 2009.

[5] CHOI, J. W., LEE, J. Joint ML estimation of frame timing and carrier frequency offset for OFDM systems employing time-domain repeated preamble. IEEE Transactions on Wireless Communications, 2010, vol. 9, no. 1, p. 311 – 317.

[6] CHENG, M., CHOU, C. Maximum-likelihood estimation of frequency and time offsets in OFDM systems with multiple sets of identical data. IEEE Transactions on Signal Processing, 2006, vol. 54, no. 7, p. 2848 – 2852.

[7] Van de Beek, J.-J., Edfors, O. S., Sandell, M., Wilson, S. K., and Börjesson, O. P., "On channel estimation in OFDM systems," 45th IEEE Vehicular Technology Conference, Chicago, Il., vol. 2, pp. 815-819, July 1995.

[8] S. Saleem, Q. Islam, Performance and Complexity Comparison of Channel Estimation Algorithms for OFDM System, International Journal of Electrical & Computer Sciences IJECS-IJENS, Vol: 11 No. 02, 2011, pp. 6-12.

[9] Coleri, S., Ergen, M., Puri, A., and Bahai, A., "Channel Estimation Techniques Based on Pilot Arrangement in OFDM Systems," IEEE Transactions on Broadcasting, vol. 48, pp. 223–229, Sept. 2002.

[10] Hou, X., Li, S., Liu, D., Yin, C., and Yue, G., "On Two-dimensional Adaptive Channel Estimation in OFDM Systems," 60th IEEE Vehicular Technology Conference, Los Angeles, Ca., vol. 1, pp. 498–502, Sept. 2004.

[11] Jang, Y.J. and Letaief, K.B. (2005), ―An efficient resorce allocation Scheme for spatial multiuser access in MIMO/OFDM systems‖, IEEE Transactions on Information Theory, Volume 53, Issue 1, Pages 107-116, January 2005.

[12] Dai , H., Molisch, A. F. and Poor, H. V. (2004), ―Downlink capacity of interference-limited MIMO systems with joint detection‖, IEEE Transactions on Wireless Communications, Volume 3, No. 2, Pages 442-453, 2004.

[13] W. Liejun," An improved Water –filling Power allocation method in MIMO OFDM System," Information technology journal, vol.10, pp 639-647,2011.

[14] C.Zeng. L.M.C. Hoo.J.M. Cioffi," Effective water filling algorithms for Gaussian multi-access channel with ISI," VTC Fall 2000, Boston, Sept. 2000.